Alginate Composite Hydrogel Bead with Multilayer Flake Structure for Dye Adsorptions

Xiaoyu Chen* **and Jie Zhu**

School of Material Engineering, Jinling Institute of Technology, Nanjing, 211169, China.
*Corresponding Author: Xiaoyu Chen. Email: chxy@jit.edu.cn.

Abstract: With the rapid development of textile industry, a large amount of dye-contaminated effluents was produced and caused serious environmental problem. To remove the dye from effluents, adsorption materials have been applied because of their relatively cheap, high efficiency, and easy handling. In this study, a novel composite hydrogel bead with unique multilayer flake structure was fabricated by alginate, acrylamide and attapulgite for dye adsorption. Acrylamide was grafted polymerization onto alginate to obtain alginate-g-poly(acrylamide). Then alginate-g-poly(acrylamide) was cross-linked by Ca^{2+} ions in present of attapulgite to form composite hydrogel bead. Scanning electron microscopy (SEM) results show that the freeze dried composite hydrogel bead has multilayer flake structure incorporating attapulgite. Fourier transform infrared spectroscopy (FTIR) and Thermo-gravimetric analysis (TGA) results indicate that acrylamide has been successfully grafted polymerization on sodium alginate. Grafting polymerization of acrylamide onto sodium alginate obviously enhances the swelling of hydrogel bead. Incorporating of attapulgite into hydrogel bead effectively enhances the adsorption capacity to methylene blue and the maximum adsorption capacity is 155.7 mg g^{-1}. Multilayer flake structure increases the adsorption area for methylene blue, but hinders the diffusion of methylene blue into the inner of composite hydrogel bead. High pH solution is beneficial to the adsorption. Pseudo-second order model and Fraundlinch model best describe the adsorption kinetic and isotherm, respectively. These results indicate that composite hydrogel bead is a promising adsorption material for dye-contaminated water treatment.

Keywords: Composite hydrogel; attapulgite; alginate; acrylamide; methylene blue; adsorption material

1 Introduction

Alginate is a water-soluble linear polysaccharide extracted from brown seaweed [1]. Alginate is biodegradable, inexpensive and non-toxic [2,3] and has been use for dye adsorption to treat dye-contaminated effluents [4-7]. Alginate is composed of (1-4)-β-D-mannuronic acid (M) and (1-4)-α-L-guluronic acid (G) units [1]. (G) units of alginate can be easily cross-linked by divalent ions such as Ca^{2+}, Ba^{2+} to form hydrogel [1].

Hydrogel can absorb and retain large amount of water without dissolution due to its hydrophilic groups and cross-linked polymer chains in structure [7]. Immersing into dye solution, dry hydrogels swell by absorbing dye solution. In this process, dye molecules diffused into the hydrogel and been adsorbed by the adsorption sites within the hydrogel [8]. High swelling and more adsorption sites in the hydrogel are beneficial for the adsorption of dye.

Increasing the number of hydrophilic groups in hydrogel is beneficial for swelling. Grafting polymerization can introduce extra chains with hydrophilic groups such as polyacrylic acid, polyamide to increase the swelling degree and further increase the adsorption capacity [9-11]. According to the reports, acrylic acid has been grafted polymerization onto alginate to prepared hydrogel. This grafting polymerization

enhanced swelling ability and adsorption ability to methylene blue [7]. Rashidzadeh [12] prepared sodium alginate-g-poly(acrylic acid-co-acrylamide)/clinoptilolite nanocomposite hydrogel and found that carboxylic and amide groups of poly(acrylic acid-co-acrylamide) were important for methylene blue adsorption.

Besides increasing the number of hydrophilic groups, increasing adsorption sites of hydrogel is also helpful to enhance the adsorption property. Incorporating clay into hydrogel to prepare composite hydrogel is an efficient method to increase the adsorption sites [12-15]. Montmorillonite [6,16], laponite [17], vermiculite [14], sepiolite [15], and attapulgite [18] have been used to prepare composites hydrogels. Attapulgite is a needle-like magnesium aluminum silicate with diameter of 20nm and length of several hundred nanometers to several micrometers [19]. Attapulgite has high specific surface area and negative charge in structure, which is beneficial to adsorb dye with positive charge [16]. Chitosan-g-poly(acrylic acid)/attapulgite composite hydrogel [20], cross-linked poly (acrylic acid-co-acrylamide)/attapulgite composite hydrogel [21] and N-succinyl-chitosan-g-polyacrylamide/attapulgite composite hydrogel [22] have been prepared to remove dye from solution.

Composite hydrogel bead prepared by alginate-g-ploy(acrylamide) and attapulgite has never been reported. In this study, acrylamide was grafted polymerization on the alginate to enhance the swelling ability of alginate and then alginate-g-ploy(acrylamide) was cross-linked by Ca^{2+} to form hydrogel bead. Meanwhile, attapulgite was incorporated into the hydrogel bead to enhance the adsorption capacity. Adsorption capacity, kinetic, and isotherm of the composite hydrogel bead for methylene blue, a well-known textile dye, was investigated.

2 Experiment Section

2.1 Materials

HCl, $CaCl_2$, Methylene blue (methylthioninium chloride $C_{16}H_{18}N_3SCl$) were all A.R. grade. Attapulgite was provided by Jiangsu dianjinshi Au soil Mining Industry Co., Ltd. Distilled water was used in all experiments. Sodium alginate was provided by Shanghai Qingxi Chemical Technology Co., Ltd.

2.2 Preparation of Composite Hydrogel Bead

Sodium alginate (1.4 g) and acrylamide (3.0 g) were dissolved in 70 g distilled water and then 0.06 g $K_2S_2O_4$ and 30 μL N,N,N',N'-Tetraethylethylenediamine were added into above solution. The solution was agitated for 3 hours under 25°C. Then certain amount attapulgite were dispersed in above gel like solution to form mixture. The mixture was dropped into 5% $CaCl_2$ solution. Hydrogel beads were formed instantaneously and were kept in $CaCl_2$ solution for 24 h in order to complete the cross-linking. In this processing, unreacted acrylamide in hydrogel beads was dissolved into $CaCl_2$ solution and be removed. Finally, hydrogel beads were rinsed with distilled water and freeze dried. Composite hydrogel beads with alginate-g-poly(acrylamide)/attapulgite mass ratios of 1:0.5, 1:1, 1:1.5, 1:1.2, 1:2.5 and 1:3 were labeled as SAA1, SAA2, SAA3, SAA4, SAA5, and SAA6, respectively. Neat alginate bead and alginate-g-ploy(acrylamide) bead were coded as SA and SAA0, respectively.

2.3 Characterization

Surface morphology of composite hydrogel bead was observed by scanning electron microscopy (SEM, SU8010, Hitachi). Structure of hydrogel was detected by smart iTR accessory of Fourier transform infrared spectroscopy (FTIR) spectrometer (Thermo Fisher Nicolet iS10). Thermo-stability was detected by TGA which was performed by heating samples to 700°C at 5 °C/min under a nitrogen flow by thermogravimetric Analyzer (STA 409 PC Luxx NETZSCH).

2.4 Swelling Measurement

Freeze dried beads were immersed in distill water. At specific time intervals, beads were taken out from water and were weighted. The swelling degree, S(t), at time t was calculated using Eq. (1), where W_t and W_d are the sample weights at time t and at the initial time, respectively.

$$S(t) = \frac{W_t - W_d}{W_d} \tag{1}$$

2.5 Dye Adsorption Capacity Measurement

Freeze dried beads (0.2 g) were immersed in 50 mL methylene blue (MB) solution of 87.4 mg L^{-1} at 25°C for 72 h. the absorbence at 664 nm of final solution was measured with UV-Vis spectrophotometer (VARIAN Cary 50). Absorbence was converted to concentration by standard curve of MB. The adsorption capacity, Q, was calculate by Eq. (2).

$$Q = \frac{(C_0 - C_e)V}{m} \tag{2}$$

where C_0 (mg L^{-1}) is the initial dye concentration of the solution, C_e (mg L^{-1}) is the equilibrium dye concentration of the solution, V (L) is the volume of the solution, and m (g) is the origin weight of the beads.

2.6 Adsorption Capacity at Different pH of Solution

SAA2 (0.1 g) was immersed into 50 mL MB solution (90.12 mg L^{-1}) with pH variation between 4 and 10 for 72 h at 25°C. The initial pH of MB solution was adjusted with 0.1 mol L^{-1} HCl aqueous solution or 0.1 mol L^{-1} NaOH aqueous solution. Adsorption capacity was calculated by Eq. (2).

2.7 Adsorption Capacity at Different Initial Concentration of MB

SAA2 (0.1 g) was immersed into 50 mL MB solution at 25°C for 72 h at initial concentration of 200, 300, 400, 500, 600, 700, 800 mg L^{-1}, respectively. Adsorption capacity was calculated by Eq. (2).

2.8 Adsorption Kinetic

SAA2 (0.4 g) was immersed into 100 mL MB solution of 87.4 mg L^{-1} at 25°C. At desired time intervals, 0.5 mL solution was taken out to detect the absorbance via UV-Vis spectrometer until the absorbance of residual solution is constant. Adsorption capacity was calculated by Eq. (2).

2.9 Adsorption Isotherm

SAA2 (0.1 g) was immersed into 80 mL MB solution at concentration of 67.18 mg L^{-1}, 84.99 mg L^{-1}, 96.49 mg L^{-1}, 105.84 mg L^{-1}, and 113.42 mg L^{-1} at 30°C for 72 h. The same procedure was conducted at 35°C and 40°C. Then 0.3 mL MB solution was taken out from the solution to detect the absorbance via UV-Vis spectrometer. Adsorption capacity was calculated by Eq. (2).

3 Results and Discussion

3.1 Preparation

Preparation process is described by Fig. 1. Acrylamide was grafted polymerization onto alginate to prepare alginate-g-ploy(acrylamide) by radical initiation at 25°C. Then alginate-g-ploy(acrylamide) solution was mixed with attapulgite and dropped into the Ca^{2+} solution. Alginate-g-poly(acrylamide) molecules in droplet was cross-linked by the Ca^{2+} in present of attapulgite. Using this facile method, composite hydrogel beads were prepared.

Grafting polymerization of acrylamide onto alginate introduces hydrophilic $-NH_2$ groups on molecular chain of alginate. $-NH_2$ groups are beneficial to the swelling and adsorption of hydrogel beads. We use $K_2S_2O_4$ and N,N,N',N'-Tetraethylethylenediamine as oxidation-reduction initiator to initiate radical grafting polymerization. $K_2S_2O_4$ is a kind of persulfate initiator which decomposes under heating to form radicals. But using $K_2S_2O_4$ and N,N,N',N'-Tetraethylethylenediamine together, $K_2S_2O_4$ decomposed at 25°C to form radicals and initiated grafting polymerization. Acrylamide monomer grafted onto alginate through produced radicals. This oxidation-reduction initiator decreased the temperature of

grafting polymerization compared to single $K_2S_2O_4$, which decreased the cost of preparation. This oxidation-reduction initiator is also easy handing.
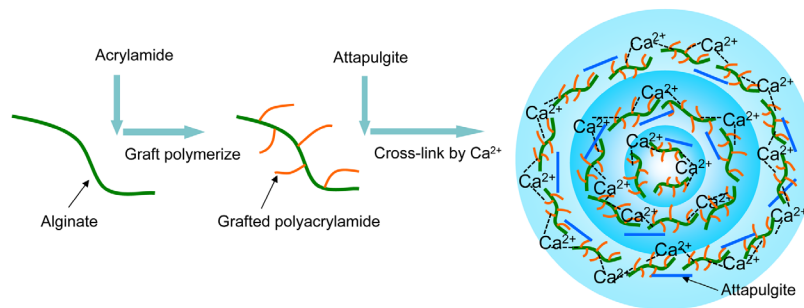

Figure 1: Schematic depiction of preparation of composite hydrogel bead

Using Ca^{2+} to cross-link alginate to form hydrogel is a simple and rapid method and has been widely investigated [2,6,23,24]. Alginate is composed of 1,4-linked β-D-mannuronic acid (M-block) and α-L-guluronic acid (G-block). G-blocks of different molecular chain of alginate can be stacked together by divalent cations such as Ca^{2+} to form "egg-box" structure [25]. These stacked G-blocks behave as cross-linking point to cross-link molecular chain of alginate to form hydrogel.

Attapulgite was incorporated into the hydrogel bead to enhance the adsorption capacity. Solely using attapulgite will cause second pollution due to the dispersion of small sized attapulgite in water. But incorporation of attapulgite into hydrogel bead can avoid this second pollution. Prepared composite hydrogel beads (SAA2) were shown in Fig. 2. Beads have smooth surface and have a diameter of about 3 mm.
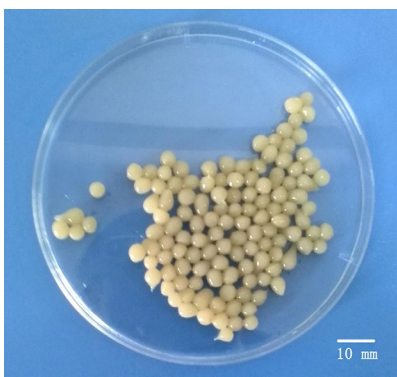

Figure 2: Photo of prepared composite hydrogel beads (SAA2)

3.2 Morphology and Structure

The surface of freeze dried hydrogel bead exist undulations (Figs. 3(A)-3(C), 3(E), 3(G), and 3(H)). These undulations maybe due to the shrink of hydrogel bead during freeze drying and increased the surface area for MB adsorption. We can see multilayer flake structure exist in composite hydrogel bead (Figs. 3(D) and 3(E) (cross-section of SAA2)). Fig. 3(F) shows that attapulgite is located in multilayer flake. This multilayer flake structure is different to reported porous structure of nature polymer adsorption materials [24,26]. Multilayer flake is formed by the cross-linked alginate molecular chain. Multilayer flake structure increased area of adsorption, which leads to high adsorption capacity to MB.

FTIR spectra of SA, SAA0, attapulgite, and composite hydrogel bead (SAA2) are shown in Fig. 4. In the peaks of spectrum of SA, 1596 cm^{-1} and 1427 cm^{-1} belongs to the anti-symmetric stretch vibration and symmetric stretch vibration of COO^- of alginate, respectively. In the peaks of spectrum of SAA0, 1668 cm^{-1} belongs to the C=O stretch vibration of -$CONH_2$ of grafted polyacrylamide. 1460 cm^{-1} belongs to the deformation vibration of -CH_2-. Peak of 1609 cm^{-1} is the combination of N-H bending vibration of -$CONH_2$ and anti-symmetric stretch vibration of COO^- of alginate. 1418 cm^{-1} belongs to the symmetric stretch

vibration of COO$^-$ of alginate. These results indicate that acrylamide was successfully grafted polymerization onto alginate. Besides the peaks of SAA0, peaks of attapulgite were appeared in the spectrum of SAA2. 3615 cm^{-1} belong to the stretching modes of hydroxyls coordinated with the magnesium in attapulgite. 3586 cm^{-1} and 3550 cm^{-1} are attributed to the symmetric and anti-symmetric stretching mode of molecular water coordinated with the magnesium at the edges of the channels of attapulgite [27]. 1028 cm^{-1} belongs to Si-O-Si stretching vibration of attapulgite [28]. These peaks reveal that attapulgite was successfully incorporated into the hydrogel bead.
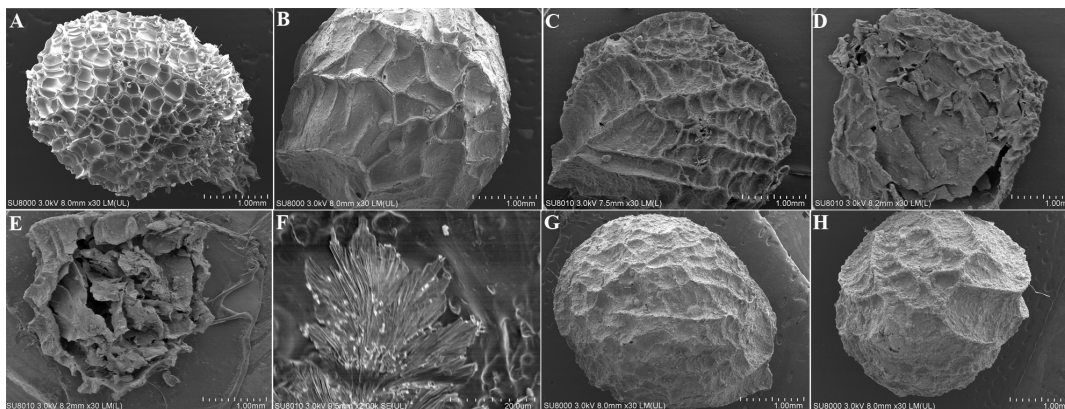

Figure 3: SEM micrographs: (A) SAA0; (B) SAA1; (C) SAA2; (D, E) cross-section of SAA2; (F) attapulgite in SAA2; (G) SAA3; (H) SAA6
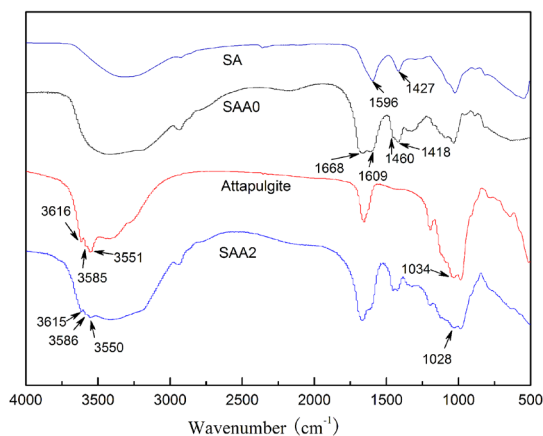

Figure 4: FTIR spectra of SA, SAA0, attapulgite, and SAA2

TGA curves for attapulgite, SAA2, SAA0, and SA are presented in Fig. 5. For attapulgite, below 100°C, the weight loss was ascribed to the removal of water which including surface water and zeolitic water of attapulgite. Above 400°C, the weight loss corresponds to the loss of coordinated water and structural hydroxyl water in attapulgite. The TGA curve of SA has a rapid weight loss between 220-270°C, which can be attributed to the decomposition of molecular chain of alginate. This rapid weight loss is accord with the reported TGA of alginate [29]. The TGA curve of SAA0 has two rapid stages of weight loss in the range of 250-310°C and 310-400°C, respectively. The first stage can be attributed to the decomposition of alginate. The second stage can be attributed to the decomposition of grafted poly(acrylamide), which is accord with the reported TGA of polyacrylamide grafted xanthan gum [30]. The two stages indicate that acrylamide has been grafted polymerization on alginate. The TGA curve of SAA2 also has two stages of weight loss which are similar to SAA0. The high residue mass of SAA2 indicate the existence of attapulgite in SAA2.
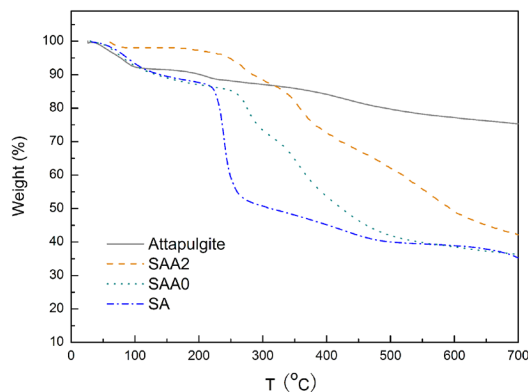
Figure 5: TGA curves of attapulgite, SAA2, SAA0, and SA

3.3 Swelling Behavior

Influence of attapulgite content on swelling degree of composite hydrogel beads are showed in Fig. 6. For the beads without attapulgite, SAA0 (alginate-g-ploy(acrylamide) hydrogel bead) has larger swelling degree than SA (neat alginated hydrogel bead), which indicate that introducing hydrophilic amine groups on sodium alginate by grafting polymerization greatly enhanced the swelling degree [31]. Introduced hydrophilic amine groups interact with water molecular to retain water in hydrogel, which increase the swelling degree. For the beads with attapulgite, swelling degree decreases with the increasing of attapulgite content. Attapulgite is located on the multilayer flake and physically filled in the network formed by sodium alginate molecular. Multilayer flakes create structural barrier which impedes the diffusion of water molecules into the inner of composite hdyrogel bead, leading to a decrease in swelling degree.
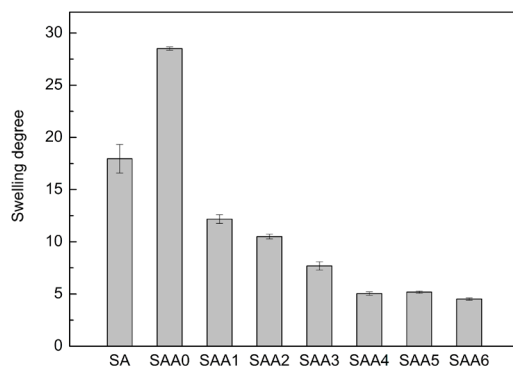

Figure 6: Swelling degree of composite hydrogel beads with different attapulgite content

3.4 Dye Adsorption Capacity

Adsorption capacities of composite hydrogel beads are shown in Fig. 7. With the increasing of content of attapulgite, the adsorption capacity first increases and then keeps nearly constant about 21 mg g^{-1}. All the composite beads have larger adsorption capacities than beads without attapulgite (SAA0). Immersed in MB solution, dry composite hydrogel swell by absorbing dye solution. In this process, MB molecules diffused into the hydrogel. Cationic MB molecules can be adsorbed by attapulgite with negative surface charge in multilayer flake structure of composite bead via electrostatic attraction. So incorporating attapulgite into hydrogel bead to form composite hydrogel bead effectively enhances the adsorption capacity to methylene blue.

But in Fig. 7, high content of attapulgite do not lead to high adsorption capacity. SAA2, SAA3, SAA4, SAA5, and SAA6 have similar adsorption capacity although the content of attapulgite is increasing. Adsorption capacities keep nearly constant about 21 mg g^{-1}. This phenomenon is correlated to

the swelling degree of SAA2, SAA3, SAA4, SAA5, and SAA6. As we mentioned above, high swelling and more adsorption sites in the hydrogel are beneficial for the adsorption of dye. With the increasing of content of attapulgite, adsorption sites are increase, which is beneficial to adsorb more MB molecules. But increasing content of attapulgite decreased the swelling degree of composite hydrogel. This has been discussed in Section 3.3. Low swelling degree decreases number of MB molecules diffused into the composite hydrogel bead, which leads to the decrease of adsorption capacity.

This can be confirmed by Fig. 8 which shows the diffusion of MB in the hydrogel bead after adsorption of 72 hours in MB solution. Cross-sections of SAA0, SAA1 and SAA2 are all blue (Figs. 8(A)-8(C)), which indicates that MB has diffused into the inner of beads. Cross-sections of SAA3, SAA4, SAA5, and SAA6 have white core (Figs. 8(D)-8(G)), which indicates that MB cannot diffuse into the inner of beads. Attapulgite in the inner of these beads cannot contact with MB and cannot further adsorb MB.

So with the increasing of content of attapulgite, adsorption capacity finally keeps nearly constant as shown in Fig. 7.
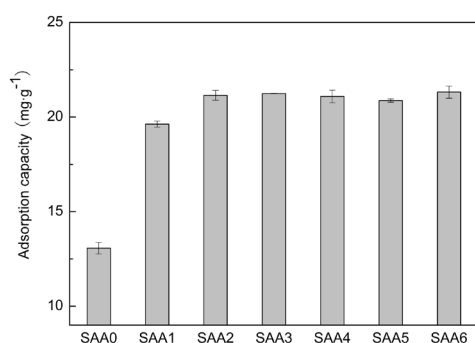

Figure 7: Adsorption capacities of composite beads with different content of attapulgite in 87.4 mg g^{-1} methylene blue solution
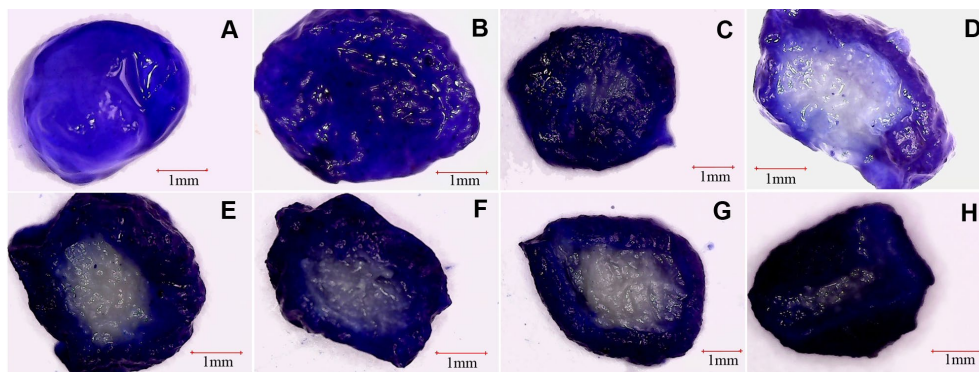

Figure 8: Cross-sections of beads with different content of attapulgite in methylene blue solution after adsorption of 72 hours. A: SAA0, B: SAA1, C: SAA2, D: SAA3, E: SAA4, F: SAA5, G: SAA6, H: SAA6 (surface)

3.5 Effects of pH on Adsorption Capacity

Fig. 9 shows the adsorption capacities of composite hydrogel bead (SAA2) in the pH range of 4-10. SAA2 has a high adsorption capacity in the pH range of 4-10 and adsorption capacity increase with the increasing of pH. The increasing of adsorption capacity could be attributed to the change of charge of attapulgite in the bead. At medium or high pH, attapulgite has negatively charged sorption sites which favor the adsorption of cationic dye such as MB via electrostatic attraction. Some isomorphic substitutions in the tetrahedral layer of attapulgite, such as Al^{3+} for Si^{4+}, develop negatively charged sorption sites (Si-O$^-$) on the surface of attapulgite [32]. But At low pH, negative charge of attapulgite decrease. There are large H$^+$ ions

in solution at low pH. Some negatively charged sorption sites are protonated by H^+ to form $Si\text{-}OH_2^+$, which decrease the negative charge sites to attract MB. Meanwhile, $-NH_2$ of grafted polyacrylamide in hydrogel bead are protonated by H^+ to form NH_3^+ which lead to the electrostatic repulsion with MB and further decrease the adsorption capacity.
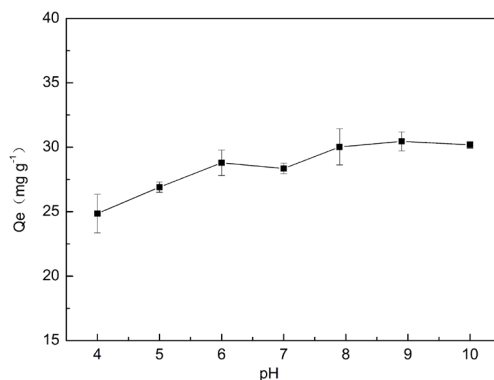

Figure 9: Effect of pH of solution on the adsorption capacity of SAA2

3.6 Effects of Initial MB Concentration on Adsorption Capacity

Adsorption capacity at different initial concentration of MB is shown in Fig. 10. Adsorption capacity increases with the increasing of initial concentration of MB. The maximum adsorption capacity is 155.74 mg L^{-1} at concentration of 700 mg L^{-1}. Maximum adsorption capacities of reported adsorption material fabricated by nature polymers are summarized in Tab. 1 (Theoretical data and experimental data). Composite hydrogel bead in this work has moderate adsorption capacity.

Table 1: Comparision of maximum adsorption capacities of different adsorbents for methylene blue

| Adsorbents	Q_m(mg g^{-1}) Cal./Exp.	References
Cellulose nanocrystal/alginate	256.4/--	[2]
Alginate/polyaspartate hydrogel gel beads	--/600-700	[24]
G-Fe_3O_4/alginate	--/37.05	[33]
Superabsorbent cellulose-clay nanocomposite hydrogel	1065/782.9	[34]
Attapulgite Nanofiber-Cellulose nanocomposite	--/11.07	[23]
PAMPS/chitosan hydrogel	--/74	[35]
Magnetic β-cyclodextrin-chitosan/ grapheme oxide	--/84.32	[36]
Macroporous composite IPN hydrogels based on poly(acrylamide) and chitosan	--/749.7	[37]
xylan/poly(acrylic acid) magnetic nanocomposite hydrogel	438.60/--	[38]
Starch-humic acid composite hydrogel	--/110	[39]
Modified cyclodextrin	--/56.5	[40]
Superabsorbent hydrogel	--/48	[41]
Attapulgite	--/51	[42]
Sodium alginate-g-poly(acrylamide)/ attapulgite composite hydrogel bead	--/155.7	This work
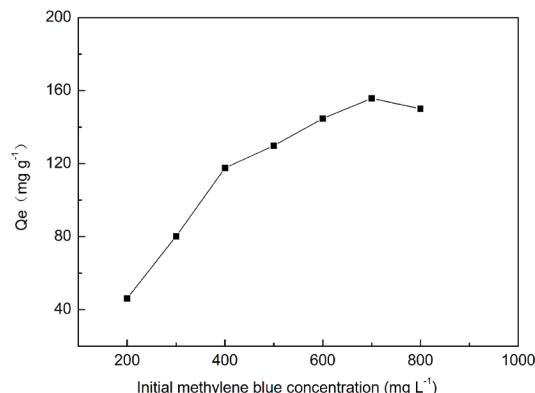
Figure 10: Effect of initial concentration of methylene blue on the adsorption capacity of SAA2

3.7 Adsorption Kinetic

Adsorption capacity of composite bead at different adsorption time ranging from 0 to 72 h at 25°C is presented in Fig. 11. Adsorption capacity increased rapidly in the initial 10 h. After 30 h, adsorption capacity was constant. Three kinetic models were used to fit these data, namely pseudo-first order (Eq. (3)) [43], pseudo-second order (Eq. (4)) [44], and intra-particle model.

$$\log(Q_{eq} - Q_t) = \log Q_{eq} - k_1 t \tag{3}$$

$$\frac{t}{Q_t} = \frac{1}{k_2 Q_{eq}^2} + \frac{1}{Q_{eq}} t \tag{4}$$

$$Q_t = K_{id} t^{1/2} + C \tag{5}$$

In these models: k_1 is the rate constant first-order adsorption (min^{-1}) [43]; Q_{eq} (mg g^{-1}) is the amount of MB adsorbed at equilibrium; Q_t (mg g^{-1}) is the amount of dye adsorbed at any time t (min); k_2 (g·mg^{-1} min^{-1}) is the second-order rate constant [44]; K_{id} (mg g^{-1} min$^{-1/2}$) is the intra-particle diffusion rate constant which describe the diffusion rates of different stages of the adsorption process; C is a constant.

Non-linear fitting of pseudo-first order and pseudo-second order models are shown in Fig. 11. Kinetic parameters are listed in Tab. 2. The low values of χ^2 and the high values of the correlation coefficient (R^2) also demonstrate a high degree of fitness for pseudo-second order model on the experimental data (Tab. 2). The pseudo second-order model assumes that the rate limiting step is chemical sorption [45]. This indicates that the adsorption of MB into composite hydrogel bead is mostly controlled by the chemisorption by exchanging or sharing of electrons between cationic dye and anion groups of composite beads [46]. The fitted curves of linear form of two kinetic models are shown in Fig. 12. Rate constants are shown in Tab. 2. The R^2 of three models also suggests that the pseudo-second order model is more suitable to describe the adsorption kinetic behavior.
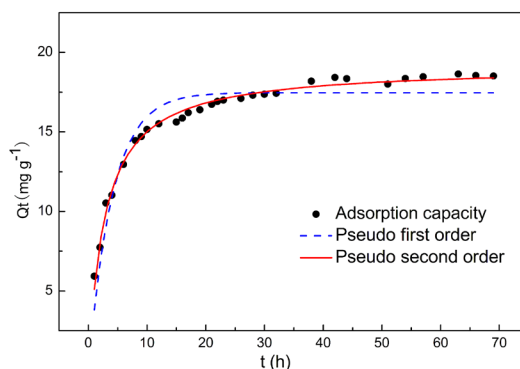

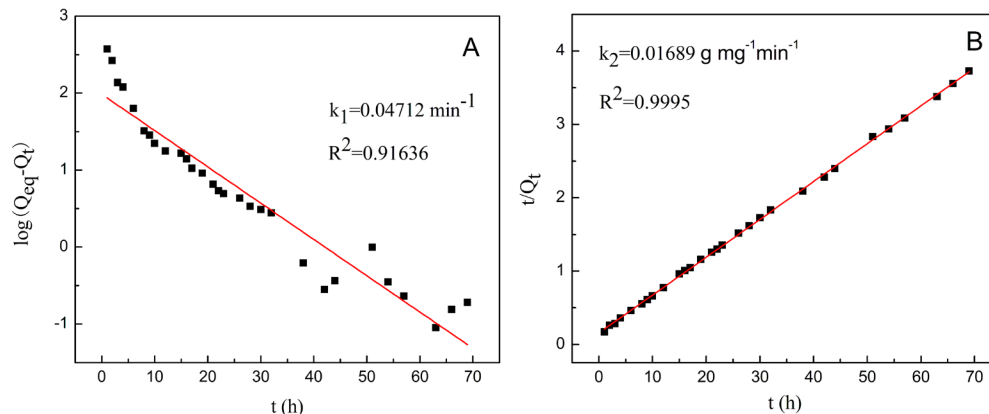**Figure 11:** Effect of contact time on the adsorption capacity of SAA2

Figure 12: Fitting curves of kinetic models of SAA2: (A) pseudo-first-order model; (B) pseudo-second-order mode

Table 2: Adsorption kinetic parameters of SAA2 for methylene blue

Model		Parameters	Value
Pseudo-first order model	Linear fitting	k_1 (min^{-1})	0.04712
		R^2	0.91636
	Nonlinear fitting	k_1 (min^{-1})	0.10648
		R^2	0.91742
		χ^2	0.91416
Pseudo-second order model	Linear fitting	k_2 (g mg^{-1} min^{-1})	0.01689
		R^2	0.9995
	Nonlinear fitting	k_2 (g mg^{-1} min^{-1})	0.01898
		R^2	0.99058
		χ^2	0.10431
Intra-particle model		$K_{id}1$ (mg g^{-1} min$^{-1/2}$)	4.44208
		$K_{id}2$ (mg g^{-1} min$^{-1/2}$)	0.98862
		$K_{id}2$ (mg g^{-1} min$^{-1/2}$)	0.15941

Adsorption involves the diffusion of MB molecules from solution into the interior of the composite hydrogel bead, so intra-particle diffusion model was used to analyze the experimental data. The intra-particle diffusion model presents multi-linearity in Fig. 13, indicating that three steps take place: a rapid first stage, a slower second and a much slower third stage until adsorption reached equilibrium. The diffusion rate constant $K_{id}1$, $K_{id}2$ and $K_{id}3$ were determined from the three slopes, respectively.

The rapid first stage is attributed to the rapid diffusion of MB from the solution to the external surface of composite hydrogel bead [46]. The second stage describes the gradual adsorption stage which MB molecules diffusion into the inner side of bead through multilayer flakes formed by alginate-g-poly(acrylamide) and attapulgite. The diffusion resistance increases which leading to a reduction in the diffusion rate. In the third stage, MB molecules diffuse into the interior of the composite hydrogel bead and the rate of diffusion slowly decreases until the adsorption reaches equilibrium.
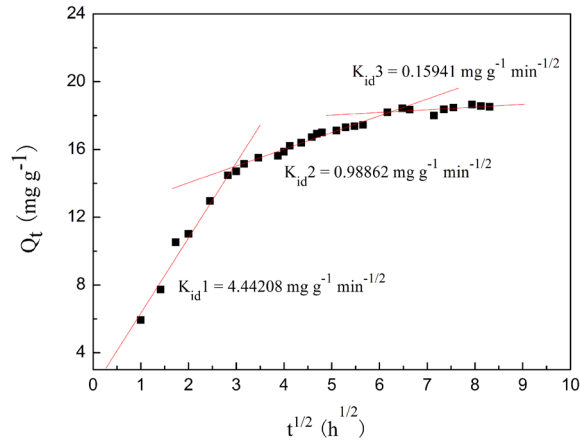
Figure 13: Fitting curves of intra-particle model of SAA2 for adsorption of methylene blue

3.8 Adsorption Isotherm

To analyze the adsorption isotherm, Langmuir model [47] and Freundlich model [48] were applied to fit the experimental data. Langmuir isotherm model assumes the adsorption is monolayer adsorption. Freundlich model is applied to describe that adsorption occurs on a heterogeneous surface.

Langmuir model can be expressed by Eq. (6)

$$\frac{1}{Q_{eq}} = \frac{1}{Q_{max}} + \frac{1}{Q_{max}b}\frac{1}{C_e} \tag{6}$$

Freundlich model can be expressed by Eq. (7)

$$\ln Q_{eq} = \frac{1}{n}\ln C_e + \ln K_F \tag{7}$$

where Q_{eq} (mg g^{-1}) is the sorption capacity at equilibrium; Q_{max} (mg g^{-1}) is the maximum adsorption capacity; C_e (mg L^{-1}) is the equilibrium concentration in the solution; b (L mg^{-1}) is the Langmuir adsorption equilibrium constant (or binding constant). K_F is the Freundlich adsorption capacity parameter, and 1/n (dimensionless) is the Freundlich adsorption intensity parameter. Higher value of K indicates higher affinity for methylene blue. 1/n is between 0.1 < 1/n < 1, indicating favorable adsorption. Langmuir and Freundlich isotherm plots are shown in Figs. 14(A) and 14(B), respectively. Parameters are exhibited in Tab. 3. The adsorption data is well fitted by Freundlich model. Values of 1/n which calculated by the Freundlich model equation are smaller than 1, which represented the favorable removal conditions.
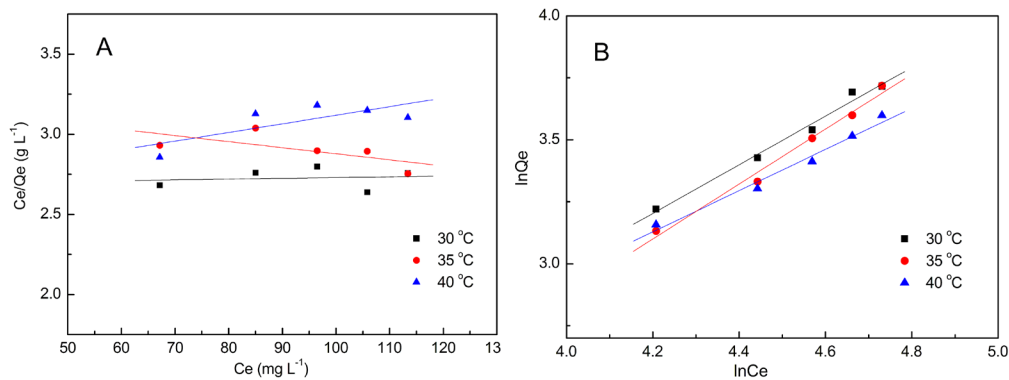

Figure 14: Fitting curves of isotherm models of SAA2: (A) Langmuir model; (B) Freundlich model

Table 3: Isotherm parameters for methylene blue adsorbed onto SAA2

T (°C)	Langmuir model			Freundlich model		
	Q_{max} (mg g^{-1})	b (L mg^{-1})	R^2	1/n	K_F (mg g^{-1})	R^2
30	2137.3595	1.744×10^{-4}	0.01688	0.9817	0.3986	0.9864
35	-263.8522	-1.164×10^{-3}	0.4550	1.1072	0.2122	0.9857
40	185.8736	2.0853×10^{-4}	0.5657	0.8317	0.6947	0.9780

4 Conclusions

Composite hydrogel bead based on alginate-g-poly(acrylamide) and attapulgite was fabricated. Multilayer flake structure was observed in the composite hydrogel bead. Grafting polymerization of acrylamide onto alginate significantly enhanced the swelling degree of hydrogel bead compared to neat sodium alginate bead. Incorporating of attapulgite into hydrogel bead effectively improved the adsorption capacity of hydrogel bead which reach 155.7 mg g^{-1} for methylene blue. High pH solution is beneficial to the adsorption. Adsorption kinetic and isotherm can be described by pseudo-second order equation and Fraundlinch equation, respectively. Due to the low cost of alginate, attapulgite and the facile preparation method, alginate-g-poly(acrylamide)/attapulgite composite hydrogel bead is a promising material using for removal of the methylene blue from water.

References

1. Liu, L., Wan, Y., Xie, Y., Zhai, R., Zhang, B. et al. (2012). The removal of dye from aqueous solution using alginate-halloysite nanotube beads. *Chemical Engineering Journal, 187,* 210-216.
2. Mohammed, N., Grishkewich, N., Berry, R. M., Tam, K. C. (2015). Cellulose nanocrystal-alginate hydrogel beads as novel adsorbents for organic dyes in aqueous solutions. *Cellulose, 22,* 3725-3738.
3. Lee, K. Y., Mooney, D. J. (2012). Alginate: properties and biomedical applications. *Progress in Polymer Science, 37,* 106-126.
4. Li, M., Elder, T., Buschle-Diller, G. (2017). Alginate-based polysaccharide beads for cationic contaminant sorption from water. *Polymer Bulletin, 74,* 1267-1281.
5. Şolpan, D., Torun, M., Güven, O. (2008). The usability of (sodium alginate/acrylamide) semi-interpenetrating polymer networks on removal of some textile dyes. *Journal of Applied Polymer Science, 108,* 3787-3795.
6. Gjipalaj. J, Alessandri, I. (2017). Easy recovery, mechanical stability, enhanced adsorption capacity and recyclability of alginate-based TiO$_2$ macrobead photocatalysts for water treatment. *Journal of Environmental Chemical Engineering, 5,* 1763-1770.
7. Thakur, S., Pandey, S., Arotiba, O. A. (2016). Development of a sodium alginate-based organic/inorganic superabsorbent composite hydrogel for adsorption of methylene blue. *Carbohydrate Polymers, 153,* 34-46.
8. Chen, X., Chen, C., Zhu, J. (2019). Facile preparation of cellulose-attapulgite nanocomposite hydrogel for dye adsorption. *Iranian Polymer Journal, 28,* 347-359.
9. Bhuyan, M. M., Chandra Dafader, N., Hara, K., Okabe, H., Hidaka, Y. et al. (2016). Synthesis of potato starch-acrylic-acid hydrogels by gamma radiation and their application in dye adsorption. *International Journal of Polymer Science, 2016,* 1-11.
10. Liu, X., Wei, Q. (2016). Removal of methylene blue from aqueous solution using porous starch-g-poly(acrylic acid) superadsorbents. *RSC Advances, 6,* 79853-79858.
11. Song, X., Chen, F., Liu, S. (2016). A lignin-containing hemicellulose-based hydrogel and its adsorption behavior. *BioResources, 11,* 6378-6392.

12.   Rashidzadeh, A., Olad, A., Salari, D. (2015). The effective removal of methylene blue dye from aqueous solutions by NaAlg-g-poly(acrylic acid-co-acryl amide)/clinoptilolite hydrogel nanocomposite. *Fibers and Polymers, 16,* 354-362.

13.   Shi, Y., Xue, Z., Wang, X., Wang, L., Wang, A. (2013). Removal of methylene blue from aqueous solution by sorption on lignocellulose-g-poly(acrylic acid)/montmorillonite three-dimensional cross-linked polymeric network hydrogels. *Polymer Bulletin, 70,* 1163-1179.

14.   Liu, Y., Zheng, Y., Wang, A. (2010). Enhanced adsorption of methylene blue from aqueous solution by chitosan-g-poly (acrylic acid)/vermiculite hydrogel composites. *Journal of Environmental Sciences, 22,* 486-493.

15.   Mahdavinia, G. R., Asgari, A. (2013). Synthesis of kappa-carrageenan-g-poly(acrylamide)/sepiolite nanocomposite hydrogels and adsorption of cationic dye. *Polymer Bulletin, 70,* 2451-2470.

16.   Liu, Y., Wang, W., Jin, Y., Wang, A. (2011). Adsorption behavior of methylene blue from aqueous solution by the hydrogel composites based on attapulgite. *Separation Science and Technology, 46,* 858-868.

17.   Marandi, G. B., Baharloui, M., Kurdtabar, M., Sharabian, L. M., Mojarrad, M. A. (2015). Hydrogel with high laponite content as nanoclay: swelling and cationic dye adsorption properties. *Research on Chemical Intermediates, 41,* 7043-7058.

18.   Wang, Y., Shi, X., Wang, W., Wang, A. (2013). Ethanol-assisted dispersion of attapulgite and its effect on improving properties of alginate-based superabsorbent nanocomposite. *Journal of Applied Polymer Science, 129,* 1080-1088.

19.   Yang, H., Wang, W., Wang, A. (2012). A pH-sensitive biopolymer-based superabsorbent nanocomposite from sodium alginate and attapulgite: synthesis, characterization, and swelling behaviors. *Journal of Dispersion Science and Technology, 33,* 1154-1162.

20.   Wang, L., Zhang, J., Wang, A. (2011). Fast removal of methylene blue from aqueous solution by adsorption onto chitosan-g-poly (acrylic acid)/attapulgite composite. *Desalination, 266,* 33-39.

21.   Wang, Y., Zeng, L., Ren, X., Song, H., Wang, A. (2010). Removal of methyl violet from aqueous solutions using poly (acrylic acid-co-acrylamide)/attapulgite composite. *Journal of Environmental Sciences, 22,* 7-14.

22.   Li, Q., Zhao, Y., Wang, L., Wang, A. (2011). Adsorption characteristics of methylene blue onto the N-succinyl-chitosan-g-polyacrylamide/attapulgite composite. *Korean Journal of Chemical Engineering, 28,* 1658-1664.

23.   Chen, X., Song, X., Sun, Y. (2016). Attapulgite nanofiber-cellulose nanocomposite with core-shell structure for dye adsorption. *International Journal of Polymer Science, 2016,* 1-9.

24.   Jeon, Y. S., Lei, J., Kim, J. H. (2008). Dye adsorption characteristics of alginate/polyaspartate hydrogels. *Journal of Industrial and Engineering Chemistry, 14,* 726-731.

25.   Grant, G. T., Morris, E. R., Rees, D. A., Smith, P. J. C., Thom, D. (1973). Biological interactions between polysaccharides and divalent cations: the egg-box model. *FEBS Letters, 32,* 195-198.

26.   Dinu, M. V., Lazar, M. M., Dragan, E. S. (2017). Dual ionic cross-linked alginate/clinoptilolite composite microbeads with improved stability and enhanced sorption properties for methylene blue. *Reactive & Functional Polymers, 116,* 31-40.

27.   Huang, J. H., Liu, Y. F., Jin, Q. Z., Wang, X. G. (2007). Spectra study on the influence of drying process on palygorskite structure. *Spectroscopy & Spectral Analysis, 27,* 408-410.

28.   Lei, Z., Yang, Q., Wu, S., Song, X. (2009). Reinforcement of polyurethane/epoxy interpenetrating network nanocomposites with an organically modified palygorskite. *Journal of Applied Polymer Science, 111,* 3150-3162.

29.   Xiao, C., Weng, L., Zhang, L. (2002). Improvement of physical properties of crosslinked alginate and carboxymethyl konjac glucomannan blend films. *Journal of Applied Polymer Science, 84,* 2554-2560.

30.   Ghorai, S., Sarkar, A., Raoufi, M., Panda, A. B., Schönherr, H. et al. (2014). Enhanced removal of methylene blue and methyl violet dyes from aqueous solution using a nanocomposite of hydrolyzed polyacrylamide grafted xanthan gum and incorporated nanosilica. *ACS Applied Materials & Interfaces, 6,* 4766-4777.

31.   Ngwabebhoh, F. A., Gazi, M., Oladipo, A. A. (2016). Adsorptive removal of multi-azo dye from aqueous phase using a semi-IPN superabsorbent chitosan-starch hydrogel. *Chemical Engineering Research and Design, 112,* 274-288.

32.   Chen, H., Zhao, J. (2009). Adsorption study for removal of Congo red anionic dye using organo-attapulgite. *Adsorption-journal of the International Adsorption Society, 15,* 381-389.

33.   Song, N., Wu, X. L., Zhong, S., Lin, H., Chen, J. R. (2015). Biocompatible G-Fe 3 O 4 /CA nanocomposites for the removal of methylene blue. *Journal of Molecular Liquids, 212,* 63-69.

34.   Peng, N., Hu, D., Zeng, J., Li, Y., Liang, L. et al. (2016). Superabsorbent cellulose-clay nanocomposite hydrogels for highly efficient removal of dye in water. *ACS Sustainable Chemistry & Engineering, 4,* 7217-7224.

35.   Gad, Y. H. (2008). Preparation and characterization of poly(2-acrylamido-2-methylpropane-sulfonic acid)/Chitosan hydrogel using gamma irradiation and its application in wastewater treatment. *Radiation Physics and Chemistry, 77,* 1101-1107.

36.   Fan, L., Luo, C., Sun, M., Qiu, H., Li, X. (2013). Synthesis of magnetic β-cyclodextrin-chitosan/graphene oxide as nanoadsorbent and its application in dye adsorption and removal. *Colloids & Surfaces B Biointerfaces, 103,* 601-607.

37.   Dragan, E. S., Lazar, M. M., Dinu, M. V., Doroftei, F. (2012). Macroporous composite IPN hydrogels based on poly(acrylamide) and chitosan with tuned swelling and sorption of cationic dyes. *Chemical Engineering Journal, 204-206,* 198-209.

38.   Sun, X. F., Liu, B., Jing, Z., Wang, H. (2015). Preparation and adsorption property of xylan/poly(acrylic acid) magnetic nanocomposite hydrogel adsorbent. *Carbohydrate Polymers, 118,* 16-23.

39.   Chen, R., Zhang, Y., Shen, L., Wang, X., Chen, J. et al. (2015). Lead(II) and methylene blue removal using a fully biodegradable hydrogel based on starch immobilized humic acid. *Chemical Engineering Journal, 268,* 348-355.

40.   Crini, G., Peindy, H. N. (2006). Adsorption of C.I. Basic Blue 9 on cyclodextrin-based material containing carboxylic groups. *Dyes and Pigments, 70,* 204-211.

41.   Paulino, A. T., Guilherme, M. R., Reis, A. V., Campese, G. M., Muniz, E. C. et al. (2006). Removal of methylene blue dye from an aqueous media using superabsorbent hydrogel supported on modified polysaccharide. *Journal of Colloid and Interface Science, 301,* 55-62.

42.   Al-Futaisi, A., Jamrah, A., Al-Rawas, A., Al-Hanai, S. (2007). Adsorption capacity and mineralogical and physico-chemical characteristics of Shuwaymiyah palygorskite (Oman). *Environmental Geology, 51,* 1317-1327.

43.   Şolpan, D., Şen, M., Kölge, Z., Güven, O. (2008). Adsorption of Apollo reactive dyes on poly(N,N dimethylamino ethylmethacrylate) hydrogels. *Radiation Physics and Chemistry, 77,* 428-433.

44.   Nakamura, T., Ogawa, M. (2013). Adsorption of cationic dyes within spherical particles of poly(N-isopropylacrylamide) hydrogel containing smectite. *Applied Clay Science, 83-84,* 469-473.

45.   Auta, M., Hameed, B. H. (2014). Chitosan-clay composite as highly effective and low-cost adsorbent for batch and fixed-bed adsorption of methylene blue. *Chemical Engineering Journal, 237,* 352-361.

46.   Zhou, C., Wu, Q., Lei, T., Negulescu, I. I. (2014). Adsorption kinetic and equilibrium studies for methylene blue dye by partially hydrolyzed polyacrylamide/cellulose nanocrystal nanocomposite hydrogels. *Chemical Engineering Journal, 251,* 17-24.

47.   Langmuir, I. (1918). The adsorption of gases on plane surfaces of glass, mica and platinum. *Journal of the American Chemical Society, 40,* 1361-1403.

48.   Freundlich, H. M. F. (1907). Über die Adsorption in Lösungen. *Zeitschrift für Physikalische Chemie, 57,* 385-470.